IMPROVED METHODS FOR GENERATION OF SIMULATED EARTHQUAKE GROUND MOTIONS

Y. Ohsaki (I), J. Kanda (II), R. Iwasaki (II),
T. Masao (III), Y. Kitada (IV), K. Sakata (V)
Presenting Author: J. Kanda

SUMMARY

The phase characteristics of earthquake accelerograms were examined and it was found that the phase difference distribution of less than 6 Hz defines the time history envelope, while the phase difference distribution is narrower in a narrow frequency band than that of whole components especially in a high frequency range. By considering these findings four improved methods for generation of simulated earthquake ground motions are proposed. A comparison of present methods with the conventional method clarifies the significant improvement in matching to the target response spectra of various damping ratios.

INTRODUCTION

It has been common to use simulated earthquake ground motions as structural inputs for earthquake resistant design of highly important structures such as nuclear power plants. Although the time history response analysis is useful and sometimes even essential to estimate the dynamic response of these complicated structures under intense earthquakes, the adequacy of simulated input motions has not been sufficiently examined.

One of discrepancies between simulated motions and real earthquake records can be seen in low damping response spectra at high frequency ranges. In other words simulated earthquake ground motions generated to match a target response spectrum of 5% damping tend to cause significantly higher responses to a system with a high natural frequency and a low damping ratio than a target response spectrum, where target response spectra of different damping ratios from 5% are defined by an empirical transforming factor (Ref. 1).

A typical example of response spectra for simulated motions generated by a conventional Sinusoidal Wave Superimposition Method (SWSM) is shown in Fig.1. Mean of 1% response spectra, $S_V(1\%)$, of ten sample motions is approximately one standard deviation higher than that of the target, where $S_V(5\%)$ is satisfactorily met to the target of 5% damping.

It is the purpose of this paper to propose improved methods for generation of simulated earthquake ground motions whose response spectra are matched to the target spectra of various damping ratios. A clue to this problem is the phase characteristics of earthquake ground motions. Manipulations of phase spectrum generation based on an examination of real earthquake records are introduced to reduce low damping response spectra at a high frequency range.

PHASE CHARACTERISTICS OF EARTHQUAKE ACCELEROGRAMS

The Fourier phase angles define the superimposing way of Fourier components

(I) Shimizu Construction Co. Ltd., Tokyo, Japan
(II) Dept. Architecture, The University of Tokyo, Japan
(III) Nuclear Power Plant Dept.,Fujita Corporation, Yokohama, Japan
(IV) Nippon Atomic Industry Group Co. Ltd., Kawasaki, Japan
(V) Nuclear Engr. Section, Toshiba Corporation, Yokohama, Japan

and affect the response spectra. Based on previous studies, two major roles of phase difference distribution, which is defined as the probability distribution of differences between Fourier phase angles of adjoining frequency components, have been revealed. One is that the phase difference distribution determines the envelope shape of time history (Ref. 2). The other is that the wider the phase differences are distributed, the higher the low damping response spectrum becomes, while 5% damping response spectrum matches the target (Ref. 3). This tendency signifies at higher frequency ranges.

In order to generate a consistent earthquake ground motion, the phase characteristics should be adequately simulated to those of real earthquake records. Therefore numerous strong seismograms were examined from the view point of phase difference distribution characteristics.

Although the phase difference distribution defines the envelope shape, the power at higher frequency ranges diminishes in most earthquake ground motion records, and so it can be imagined that the significance of frequency range for defining the envelope shape would not be the same.

The relationship between the envelope shape and significant frequency bands was clarified by calculating the ratio of the maximum acceleration of low pass filtered record to that of the original record for 82 real earthquake accelerograms. The mean value and standard deviation for the ratio were plotted against the cut-off frequency of filter in Fig. 2. The low pass filter used in this study was a rectangular shape. As seen in the figure, components of less than 3Hz to 4Hz are not sufficient to represent the original wave shape in terms of maximum acceleration and those of less than 6Hz to 8Hz seem to be fairly enough to respresent a similar wave form to the original.

Then the phase difference distributions of band pass filtered accelerograms were examined. The standard deviation of phase differences for band passed record $\sigma^{L}_{\Delta\phi}$ was normalized by that of the original one $\sigma^{T}_{\Delta\phi}$ and plotted against the center frequency of the frequency band, f_m, with band width B_f in Fig. 3. When $\sigma_{\Delta\phi}$ was calculated, the range of the phase difference distribution was adjusted beforehand for the mean value of phase difference to be situated at the center of phase difference range. As seen in Fig. 3, the ratio $\sigma^{L}_{\Delta\phi}/\sigma^{T}_{\Delta\phi}$ decreases when the band width B_f decreases and when the center frequency f_m increases. This tendency suggests that the earthquake ground motion should be generated by specifying the phase characteristics whose phase differences are distributed narrower in narrow frequency bands than that of whole frequency components. This means that narrow band components are more concentrated in time domain than the whole time history envelope.

IMPROVED METHODS FOR SIMULATION

The conventional SWSM or the phase difference method as its alternative (Ref. 2) for generation of simulated earthquake ground motions, based on the random phase postulation, is convenient for the probabilistic approach since any number of simulated samples can be generated with various combinations of Fourier phases. However the low damping response spectra, e.g. $S_V(1\%)$, of simulated motions by SWSM with $S_V(5\%)$ matched to the target, tend to be significantly higher than the target of 1% damping as shown in Fig. 1.

Several alternative methods have been developed to minimize the difference between the response spectra of simulated motions and those of the target for different damping ratios, concentrating on the manipulation of the phase characteristics. Four improved methods are summarized and proposed in this section. The sampling time in this study was taken to be 0.01sec., and the Duhamel integral was used for numerical integration. Fitting iteration was

performed for the 5% damping real velocity response spectra to the target Ohasaki spectra, of the earthquake magnitude M = 7 and the epicentral distance Δ = 20 (km).

Beat Wave Superimposition Method (BWSM)

This method (Ref. 4) was motivated from the fact that band pass filtered accelerograms tend to appear like a few repetition of beat waves. The i-th element wave (beat wave) is defined as,

$$y_i(t) = \sum_j a_j \cos(2\pi\{ f_i + \Delta f_i(j-1) \} t + \phi_{ij}) \qquad (1)$$

where f_i is the lowest frequency in the i-th frequency band, Δf_i is the frequency increment in the i-th frequency band and ϕ_{ij} is the j-th phase angle for the j-th component wave in the i-th frequency band. Δf_i is chosen to be greater than the frequency increment Δf (= $1/T_d$ where T_d is the duration of motion) used in the Fourier transform. The amplitude of component wave aj is determined by the iteration to meet the target response spectrum.

The simulated motion in this method is defined as the superimposition of $y_i(t)$ with multiplication of specified envelope function in a similar way to SWSM, i.e.,

$$y(t) = e(t) \sum_i y_i(t) \qquad (2)$$

In order to reduce the low damping response spectra, while the 5% response spectrum is matched to the target, ϕ_{ij} values were generated from a narrow rectangular phase difference distribution for each element wave. An example of time history and response spectra for a simulated motion is shown in Fig. 4.

Partial Impulse Phase Method (PIPM) (Ref. 3)

It is well-known that the impusle produces less difference for the maximum response of dynamic system with various dampings than that by the stationary wave which allows the resonance to develop. Therefore the most effective way to reduce the low damping response spectra, while the 5% response spectra are kept the same, is to utilize the impulse phase. However the time history of impulse can not be representative of an earthquake ground motion.

A simple practical solution to this can be obtained by using the impulse phase partially in a limited frequency range, e.g. between 6Hz to 14Hz. The Fourier amplitudes are determined in an iterative way to meet a target response spectrum, e.g. $S_V^T(5\%)$ with the Fourier phase angles determined from randomly generated phase differences according to a distribution specified by an envelope form (the phase difference method) in other frequency ranges.

An example is shown in Fig. 5. The impulse phase characteristics can hardly be seen in the time history but clearly recognized in $S_v(1\%)$ of the frequency range between 6Hz to 14Hz.

Narrow-band Phase Difference Method (NPDM) (Ref. 3)

Since the width of the phase difference distribution determines the ratio of $S_V(1\%)$ to $S_V(5\%)$ and at the same time relatively lower frequency components determine the envelope form, it was attempted to apply different phase difference distributions to respective frequency bands. Namely the width of phase difference distribution in high frequency ranges was deliberately reduced in

order to reduce $S_V(1\%)$ without loosing the $S_V(5\%)$ match to $S_V^T(5\%)$ and without changing the envelope form.

An example generated by NPDM is shown in Fig. 6. The 1% damping response was reduced to meet the target better than that of the conventional SWSM, although the response value around the boundary of frequency bands is still rather higher than the target.

Algebraic Function Phase Method (AFPM)

As seen in Fig. 5, the impulse phase seems to provide the least and smooth $S_V(1\%)$, where the impulse phase means zero phase difference. It was intended, in this method, to expand the impulse-like wave in time domain by applying an algebraic function to the Fourier phase. A successful example was demonstrated by the following function for the Fourier phase angle $\phi(f)$;

$$\phi(f) = \alpha f + d\, e^{-\kappa f} - d \qquad (3)$$

where $\alpha = -24$ (rad/Hz), $d = 160$ (rad), $\kappa = 0.255$ (1/Hz) were chosen to give a best fit to both 1% and 5% damping target response spectra. The result is shown in Fig. 7.

The Fourier phase for less than 6Hz and greater than 35Hz were randomly generated as SWSM to hold the time history envelope form. The fitness of both $S_V(5\%)$ and $S_V(1\%)$ to the target is almost perfect in a frequency range of our concern, say between 6Hz to 20Hz.

COMPARISON OF SIMULATED EARTHQUAKE GROUND MOTIONS BY VARIOUS METHODS

As a practical application example, the floor response spectra for simulated earthquake ground motions by the methods mentioned above were compared. A lumped mass model with a sway-rocking spring at the bottom was used to represent a typical BWR type nuclear power plant building as shown in Fig. 8.

Computed floor response spectra of 1% damping at nodal point 1, which corresponds to the upper surface of the base mat, are shown for motions by BWSM and PIPM in Fig. 9(a) and those by NPDM and AFPM in Fig. 9(b) in comparison with mean ± one standard deviation range for floor response of ten sample motions by SWSM. A considerable reduction in a frequency range around 10Hz can be recognized when present methods were applied versus the case of the conventional SWSM.

As final results, a comparison of maximum acceleration, maximum velocity, response spectra matching, where $E_{rr}(h)$ indicates the root mean square error for response spectra of damping h to the target in respective frequency range and maximum floor response acceleration values is summarized in Table 1 for simulated motions.

CONCLUSION

Improved methods to generate a simulated earthquake ground motion, whose response spectra are matched to the target spectra for various damping ratios, are proposed and compared.

They are Beat Wave Superimposition Method, Partial Impulse Phase Method, Narrow-band Phase Difference Method and Algebraic Function Phase Method. When $S_V(5\%)$ is satisfactorily met to the target, PIPM provides a minimum of $S_V(1\%)$ and AFPM provides a best fit to the target $S_V^T(1\%)$, although both methods take rather artificial Fourier phase characteristics. BWSM and NPDM also give

better fit to the target $S_V^T(1\%)$ than that of the conventional SWSM or the phase difference method.

Since the floor reponse value of low damping at around 10Hz of simulated earthquake ground motions generated by SWSM tends to be extraordinarily higher as expected from their $S_v(1\%)$, significant reduction provided by motions generated by the present improved methods should create rational reduction of earthquake design load on high frequency low damping systems such as piping systems or equipments in plant buildings. Any of present four methods could be a useful alternative to the conventional method to generate simulated earthquake ground motions for earthquake resistant design.

REFERENCES

(1) Hisada,T., Ohsaki,Y. et al,"Design Spectra for Stiff Structures on Rock", Proc. 2nd Int. Conf. Microzonation, vol.III, San Francisco, Nov.1978.
(2) Ohsaki,Y.,"On the Significance of Phase Content in Earthquake Ground Motions", Earthq. Eng. Str. Dyn. vol.7, 1979, pp 427-439.
(3) Kanda,J. et al,"Generation of Simulated Earthquake Ground Motions Considering Target Response Spectra of Various Damping Ratios", Proc. 7th SMiRT,vol.K(a), Chicago, Aug.1983, pp 71-79.
(4) Kitada,Y. et al,"Simulated Earthquake Ground Motions by Gauss Wave Superimposition Method", Proc. 7th SMiRT, vol.K(a), Chicago,Aug.1983, pp 53-61.

Table 1 Comparison of Simulated Earthquake Ground Motions by Various Methods

Methods	a_{max} (Gal) / v_{max} (kine)	$E_{rr}(5\%)$ (%)	$E_{rr}(1\%)$ (%) Total	$E_{rr}(1\%)$ (%)	Max.floor response (Gal) at nodal point 1
				0.5<f<6 Hz	0.08<T<0.16 sec
				6<f<12	0.05<T<0.08
				12<f<20	
SWSM	317.0* / 12.1*	4.1*	35.8*	21.1* / 25.3* / 36.2*	2950* / 1480*
BWSM	240.0 / 11.5	2.8	11.9	14.8 / 9.7 / 10.8	2430 (0.82) / 1300 (0.88)
PIPM	389.4 / 12.2	5.1	31.2	26.4 / 21.8 / 38.1	1480 (0.50) / 1650 (1.11)
NPDM	252.2 / 10.6	2.5	17.4	26.8 / 14.0 / 10.5	1950 (0.66) / 910 (0.61)
AFPM	222.4 / 12.3	4.1	14.1	26.9 / 2.0 / 3.8	2410 (0.82) / 1120 (0.76)

note: Values with * indicate those of average of ten sample motions and ( ) indicates the ratio to SWSM.

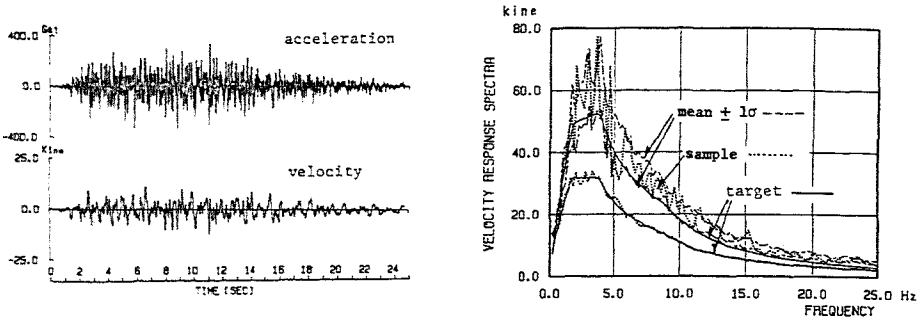

Fig. 1 Time histories and response spectra of 1% and 5% damping for simulated earthquake ground motions of M=7, Δ=20km by SWSM

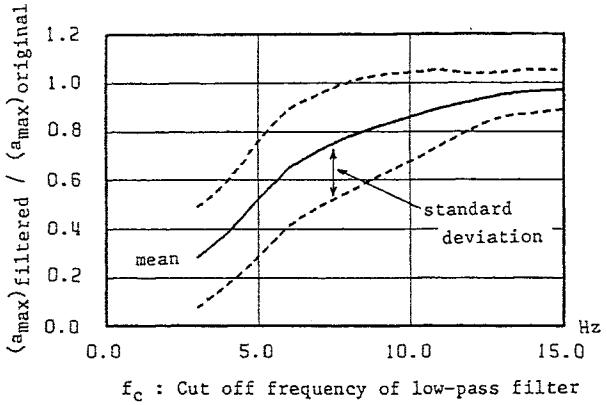

f_c : Cut off frequency of low-pass filter

Fig. 2 Mean and standard deviation of the ratio between maximum acceleration of low pass filtered wave and that of the original earthquake record with cut-off frequency f_c

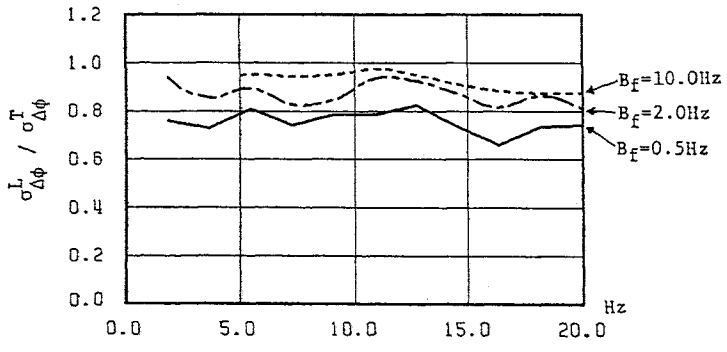

f_m : Center frequency of band-pass filter

Fig. 3 Ratio between standard deviation of phase differences for band-pass filtered wave and that of the original earthquake record with center frequency f_m

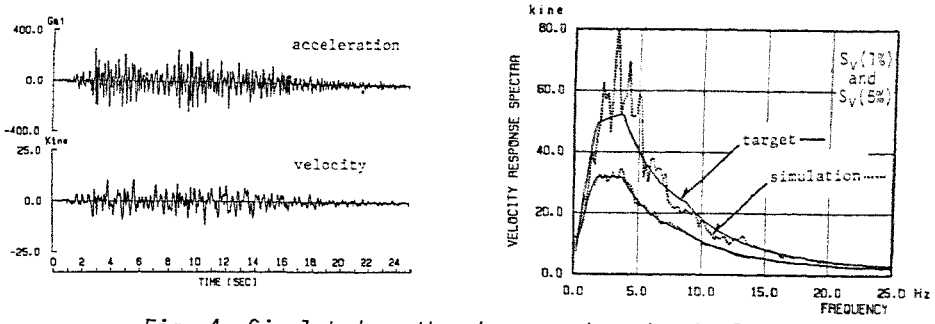

Fig. 4 Simulated earthquake ground motion by BWSM

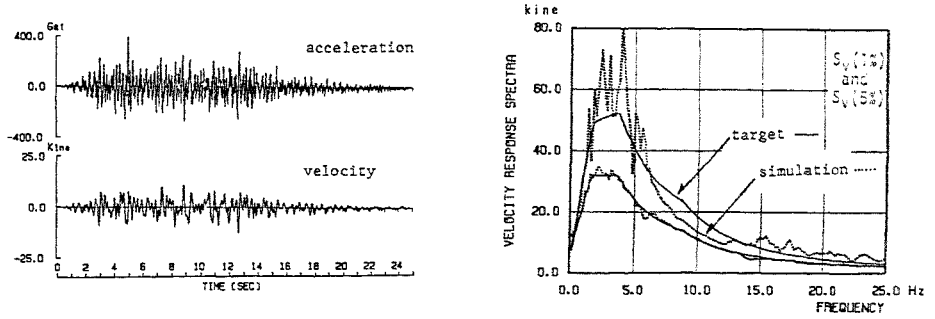

Fig. 5 Simulated earthquake ground motion by PIPM

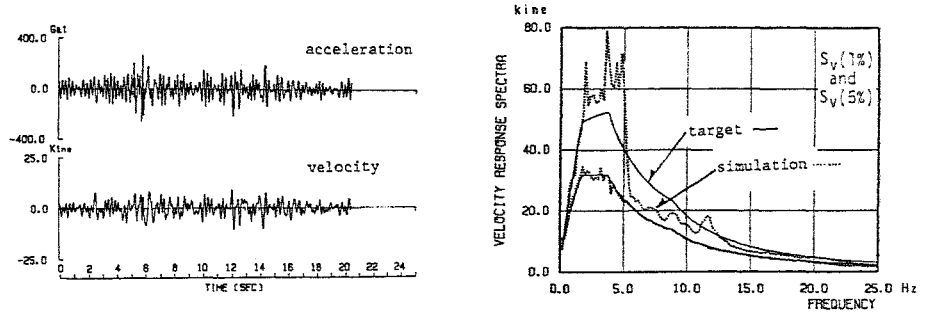

Fig. 6 Simulated earthquake ground motion by NPDM

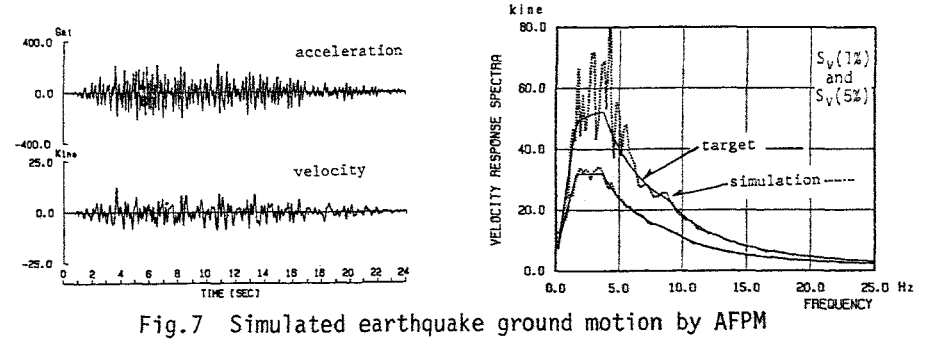

Fig.7 Simulated earthquake ground motion by AFPM

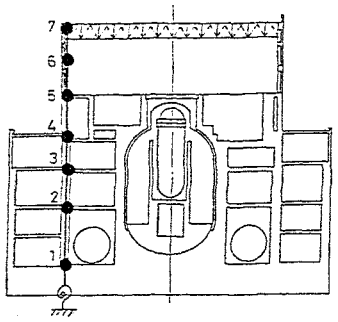

Fig. 8 Lumped mass model for a BWR Mark I type nuclear power plant

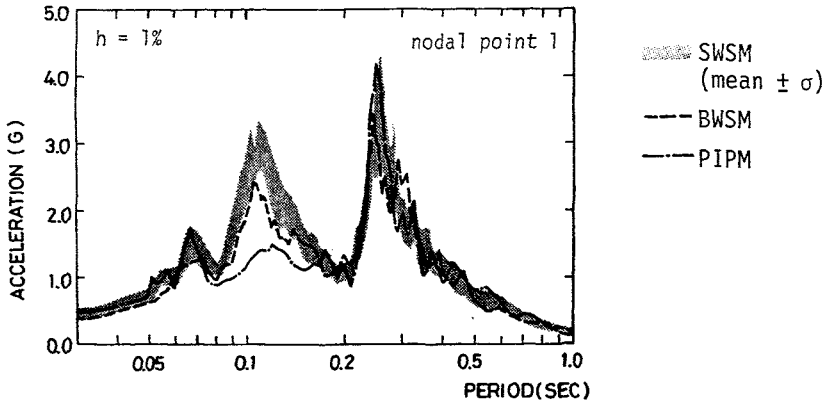

(a) comparison of BWSM, PIPM and SWSM

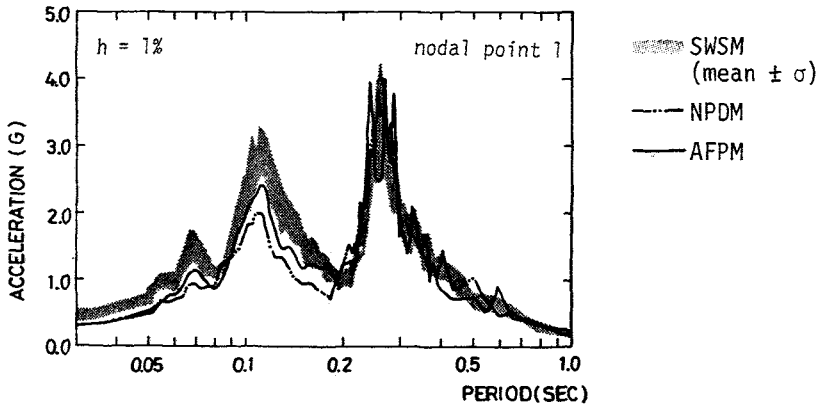

(b) comparison of NPDM, AFPM and SWSM

Fig. 9 Floor response spectra of simulated motions